Available online at www.sciencedirect.com
SCIENCE DIRECT®
Control Engineering Practice 13 (2005) 1195–1206
CONTROL ENGINEERING PRACTICE
www.elsevier.com/locate/conengprac

Feedback control of Hodgkin–Huxley nerve cell dynamics

Flavio Fröhlich[1], Sašo Jezernik*

Automatic Control Laboratory, Swiss Federal Institute of Technology (ETH Zürich), Physikstrasse 3, 8092 Zürich, Switzerland

Received 9 January 2004; accepted 5 October 2004
Available online 24 November 2004

Abstract

Nerve cells communicate by generation and transmission of short electrical pulses (action potentials). A cascaded feedback control scheme consisting of an optimal controller (model predictive control, MPC) and a state feedback controller to control the time-courses of the biophysical state variables underlying action potential generation was developed and evaluated in simulations. The control scheme was shown to provide new means for action potential generation, suppression of oscillations and blockage of action potential transmission. These new theoretical developments could represent a starting point for the design of new closed-loop electrical stimulation systems for patients suffering from different nerve system dysfunctions.

Keywords: Applied neural control; Neural dynamics; Nonlinear control; Optimal control; Medical applications

1. Introduction

The nervous system is constituted by a large number of highly interconnected nerve cells, which represent the basic biological computational units (Kandel, Schwartz, & Jessel, 2000). Separation of ionic charge along the cell membrane causes a difference in electrical potential across the cell membrane (membrane voltage). Nerve cells receive electrical input signals from other nerve cells via thread-like extensions of the cell membrane called dendrites. Depending on the spatio-temporal distribution of the input currents that depolarize the membrane voltage, firing threshold (sufficient membrane voltage depolarization) can be reached and an action potential (AP) triggered. APs are stereotyped, all-or-none electrical transient deflections of the membrane voltage from its resting value at electrochemical equilibrium. An AP is generated at the initial segment of the nerve cell's output branch called axon and propagates to the synaptic contacts at the end of the axon, the locations where the cell communicates with other cells. Two types of synapses exist, gap junctions that allow direct and fast communication between cells by means of direct ionic current flow, and chemical synapses, where a presynaptic AP triggers the excretion of neurotransmitters (chemical messengers). These in turn directly or indirectly open ion channels in the postsynaptic neuron generating an electrical signal.

The Hodgkin–Huxley (HH) equations (Hodgkin & Huxley, 1952) represent a phenomenological model of AP generation in nerve cells as a function of a given current stimulus. Electrical stimulation of nerve cells with rectangular current pulses simulates dendritic activity and allows artificial generation of APs. Electrical stimulation with current pulses has a range of clinical applications, as for example, activation of muscles by stimulating the motor nerve cell fibers innervating muscles or activation of different sensory-motor areas in the brain or spinal cord (for example, deep brain stimulation for Parkinson patients).

*Corresponding author. BERATA AG, Engineering Consulting, Schaeferweg 16, 4057 Basel, Switzerland. Tel.: +41 13507494; fax: +41 616388699.
E-mail address: jezernik@control.ee.ethz.ch (S. Jezernik).
[1]*Present address*: Computational Neurobiology, University of California San Diego, 9500 Gilman Drive, La Jolla, CA 92093-0357, USA.

0967-0661/$ - see front matter © 2004 Elsevier Ltd. All rights reserved.
doi:10.1016/j.conengprac.2004.10.008

However, such a feedforward stimulation scheme (open-loop delivery of current pulses) cannot be used to control the time-course of the state variables describing the nerve cell dynamics. A direct control of the physiological state of nerve cells allows this and offers new means of control/modulation of response characteristics of neural circuits (e.g. modulation of reflex gain). This represents a conceptually new approach to nerve cell stimulation, which to the knowledge of the authors, has not been investigated before. To design controllers allowing dynamic time-course control of biophysical state variables, advanced control algorithms are required, since inherent nonlinearities and biological constraints limit the application of linear feedback control strategies. The nonlinearities of HH nerve cell dynamics require nonlinear control strategies to achieve efficient and precise control. Furthermore, such a controller will eventually interact with biological tissue, which is sensitive to disturbances. It is thus important to use a controller generating an optimal stimulation signal which induces changes of state variables as they would arise from synaptic interaction between the nerve cells. Satisfying these constraints might also minimize adaptation of the nerve cell to the stimulation current and thus prevent a decrease in stimulation efficiency.

In the work presented here, a feedback control scheme to achieve time-course control of the opening and closing of the ion channels in the nerve cell membrane was devised and evaluated in simulations. An optimal controller for sodium activation and inactivation which describe the state of the sodium channels responsible for AP generation was combined with a state feedback controller. Model predictive control (MPC) was chosen as an optimal control paradigm using membrane voltage as control signal. By applying MPC, it was possible to influence the shape of the resulting control signal via tunable controller parameters, and to take into account biophysical constraints on the input signals and state variables. In the cascaded control scheme, the output of the MPC block constituted the input to the state feedback controller, which computed the required current to be injected into the cell.

From a biomedical engineering perspective, the control schemes described in this paper are expected to lead to improvements in existing functional electrical stimulation schemes. Possible applications are blocking of nerve cell firing and control of neural oscillation (Fröhlich & Jezernik, 2004), as well as neuromodulation.

The remainder of this manuscript is organized as follows. First, the HH model which represents the controlled plant is introduced. Then the state feedback controller for control of the membrane voltage and the cascaded controller design (comprising state feedback and MPC controllers) are presented. Next, the simulation results of the developed controllers applied to control of nerve cell dynamics are shown. Feedback annihilation of AP propagation, an additional application, is presented as well. The manuscript is concluded by a discussion.

2. Methods

2.1. Single compartment HH model

The HH equations are comprised of four coupled, nonlinear differential equations describing the temporal evolution of the membrane voltage V in dependence of an externally injected current I_{inj} in a spatially localized axonal compartment. Eq. (1) is derived by summing all the currents (ionic, capacitive, and external) across the cell membrane leading to an electrical equivalent circuit shown in Fig. 1.

$$C_m \frac{\mathrm{d}V}{\mathrm{d}t} = G_{\mathrm{K}} n^4 (E_{\mathrm{K}} - V) + G_{\mathrm{Na}} m^3 h (E_{\mathrm{Na}} - V) + G_m (V_{\mathrm{leak}} - V) + I_{\mathrm{inj}}. \quad (1)$$

The current formed by the flow of potassium ions is determined by a maximal potassium conductance G_{K}, an ionic battery E_{K} expressing steady-state potassium ion separation, and activation n describing the dynamics of potassium channel opening. Similarly, sodium ion current is modeled with a maximal sodium conductance G_{Na}, an ionic battery E_{Na}, and activation and inactivation variables m and h which describe the state of the voltage-dependent sodium channels. The remaining ion currents are collectively modeled by a leakage current (conductance G_m, ionic battery V_{leak}). Furthermore, a capacitive current is included since the cell membrane effectively separates charge (capacitance C_m). The activation and inactivation of ion channels are continuous variables which describe the macroscopic behavior of all channels of a given type in the membrane patch considered (Koch, 1999). The individual channel can be

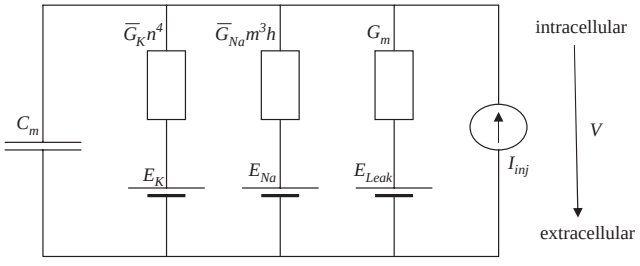

Fig. 1. Equivalent electric circuit modeling ionic current flow across nerve cell membrane as described by HH equations. The total current is the sum of a capacitive current (capacitance C_m), sodium and potassium currents, a leakage current, and the externally injected current (I_{inj}). The voltage dependent permeabilities of the ion channels are modeled as voltage dependent conductances, whereas the equilibrium potentials are modeled as constant voltage sources.

described by a binary stochastic variable which assumes either "closed" or "open" state. Potassium activation n, sodium activation m and sodium inactivation h are thus dimensionless state variables which take on continuous values between zero and one representing the fraction of channels in the corresponding state. Their dynamics are modeled with first-order differential equations listed in Eq. (2). The parameters α_n, β_n, α_m, β_m, α_h, and β_h are rate constants of the ion channel state transitions. They depend on membrane voltage V in a nonlinear manner (Hodgkin & Huxley, 1952).

$$\begin{aligned}\frac{dn}{dt} &= \alpha_n(V)(1-n) - \beta_n(V)n,\\ \frac{dm}{dt} &= \alpha_m(V)(1-m) - \beta_m(V)m,\\ \frac{dh}{dt} &= \alpha_h(V)(1-h) - \beta_h(V)h.\end{aligned} \tag{2}$$

These equations can be expressed as

$$\frac{1}{\tau_y}\frac{dy}{dt} = y - y_\infty, \tag{3}$$

where y is the (in-)activation variable, $\tau_y(V)$ is the corresponding time constant and $y_\infty(V)$ is the steady-state value for a given voltage V. Fig. 2 shows plots of τ_y (Panel A) and y_∞ (Panel B) as a function of V.

When the injected current I_{inj} is a rectangular pulse, two qualitatively different behaviors for the time course of the membrane voltage can arise. For low amplitude, short duration pulses, a slight transient deflection from the equilibrium can be observed (Figs. 3A–D). However, if a certain threshold is exceeded, an action potential is triggered (Figs. 3E–H) since enough sodium channels open so that an increase of sodium ion influx into the cell depolarizes the cell and further causes even more sodium channels to open. This positive feedback reaction responsible for AP peak generation is counterbalanced by two mechanisms. First, sodium channels get inactivated, which prevents them from opening again for a certain time. Second, there is a delayed outflux of potassium ions forcing the membrane voltage back to its resting value (repolarization). For a step current of sufficient amplitude, the HH neuron responds with a train of action potentials, which corresponds to a stable limit cycle (Fig. 4).

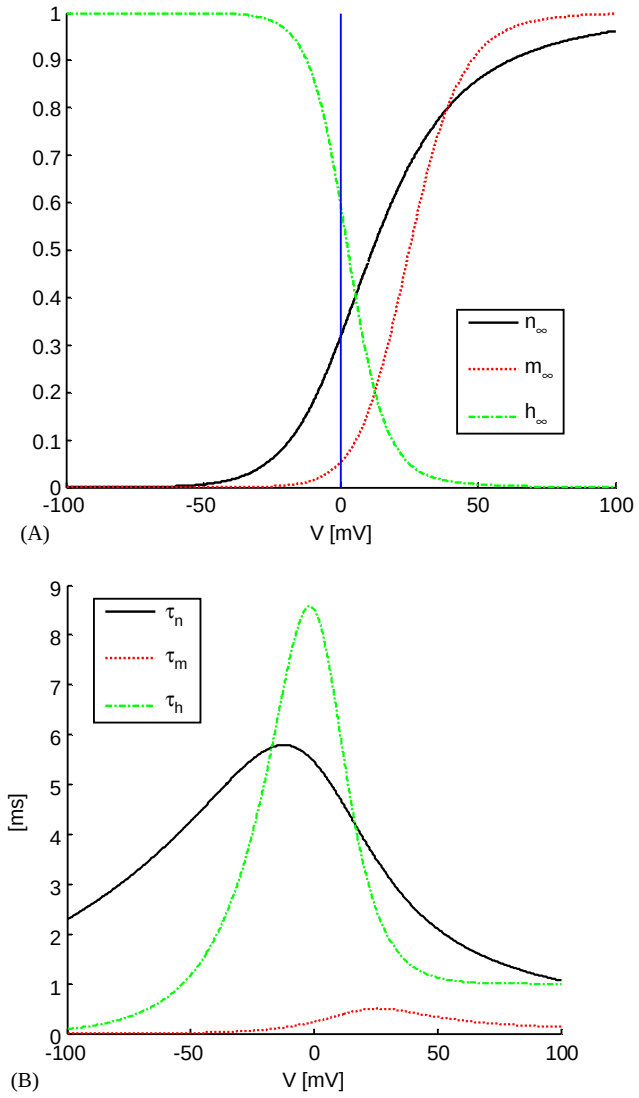

Fig. 2. The steady-state values (A) and time constants (B) for differential equations describing the state of the ion channels in the HH model neuron as a function of the membrane voltage V. Potassium activation n, sodium activation m, and sodium inactivation h describe the fraction of open potassium channels, open sodium channels, and sodium channels which are not inactivated, respectively.

2.2. Multicompartment model

The original HH model given by Eqs. (1) and (2) describes the temporal dynamics of a space-clamped axon where no spatial dynamics occur. In a more realistic model, the spatial spread of an action potential along the axon has to be considered. Action potentials propagate along the axon by currents exciting neighboring regions. In the most general case, the dynamics of the membrane voltage as a function of time and space is described by a partial differential equation of the form of a reaction-diffusion equation (Koch, 1999). Instead of numerically solving this equation, a usual approach is to divide the axon into discrete compartments (Fig. 5), which model the regeneration sites of the action potential (McNeal, 1976). At these sites (nodes of Ranvier) the axon is in direct contact with its extracellular environment, and the nodal currents can be modeled as in the HH model. The compartments are linked together by a coupling conductivity. The total current flowing into a given compartment j can be approximated by

$$I_j = G_a(V_{j-1} - 2V_j + V_{j+1}), \tag{4}$$

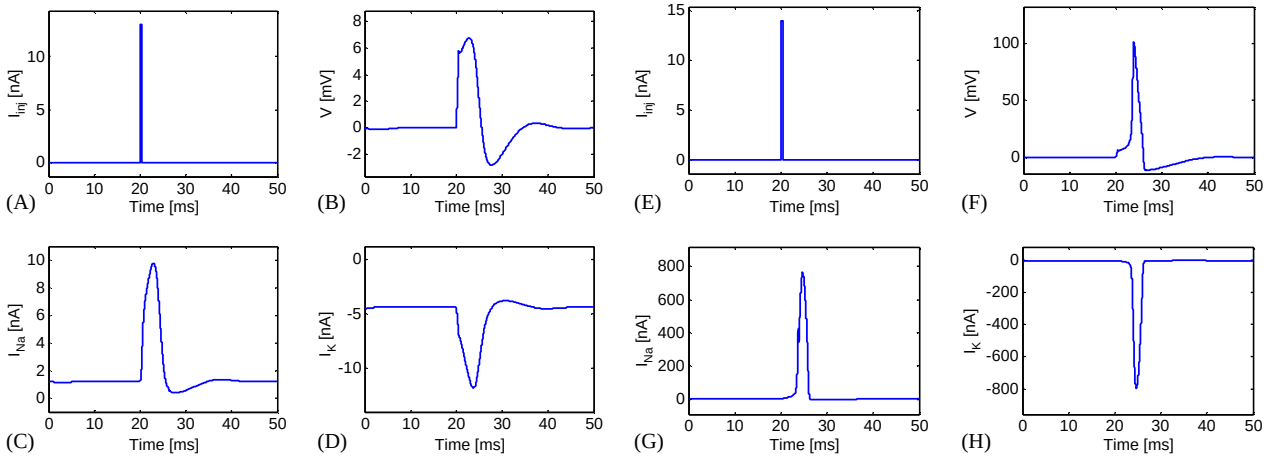

Fig. 3. Response of HH model to rectangular current pulse injection. Injected current (A, E), membrane voltage (B, F), sodium current (C, G), potassium current (D, H). Left: Subthreshold stimulation: the small injected current caused a minor deflection of the membrane voltage from its resting value and was not sufficient to trigger the positive feedback cycle responsible for an action potential generation (membrane voltage peak <8 mV). Right: Suprathreshold stimulation: the delayed potassium current could not immediately balance the inflowing sodium current, which has transiently depolarized the nerve cell. The result was a full-blown action potential (membrane voltage peak >100 mV).

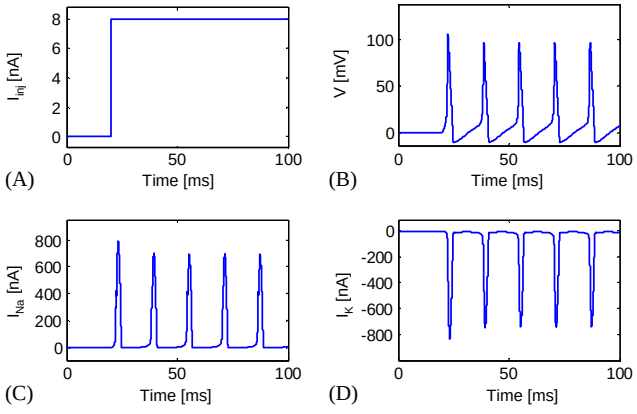

Fig. 4. Response of the HH model to a suprathreshold injection of a depolarizing current: (current step $I_{inj}=8$ nA). Injected current (A), membrane voltage (B), sodium current (C), potassium current (D). A train of action potentials with constant spiking frequency is triggered. In phase space, this oscillation corresponds to a stable limit cycle.

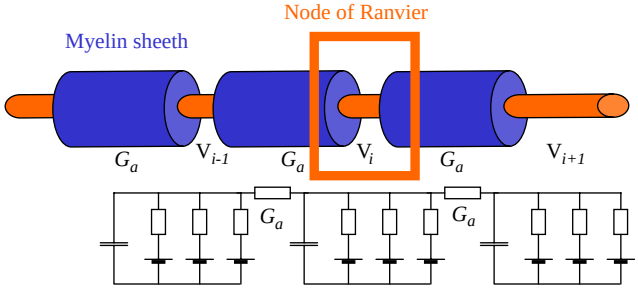

Fig. 5. Multicompartment HH model of myelinated axon. At the nodes of Ranvier, ions flow across the cell membrane allowing regeneration of a propagating action potential. The local dynamics are modeled as in the case of the single compartment model. The compartments are linked together by axonal segments, which are insulated by a myelinated sheath. Due to the insulation there is only very little current flowing across the cell membrane, therefore the compartments are connected by a coupling conductance G_a.

where G_a denotes the coupling conductivity and V_{j-1}, V_j, and V_{j+1} the membrane voltages in the corresponding compartments. Such a model consisting of 10 compartments was used to test the applicability of the control schemes to setups, where spatial propagation of APs was considered (possible application: blocking of AP propagation).

2.3. State feedback controller for control of membrane voltage

To enable feedback control of the membrane voltage the following controller design was used. Since the differential equation governing the dynamics of the membrane voltage V (Eq. (1)) is nonlinear in the state variables m, h, and n, it was first transformed into an equivalent linear differential equation by applying feedback linearization method (Khalil, 2002). This enabled the design of a state feedback controller C_1 (to control the membrane voltage) with output I_{inj} for tracking of a given membrane voltage reference time-course V_{ref}.

I_{inj} is then given by:

$$\begin{aligned} I_{inj} = & -G_K n^4 (E_K - V) \\ & - G_{Na} m^3 h (E_{Na} - V) \\ & - G_m (V_{leak} - V) \\ & + C_m (\dot{V}_{ref} + K(V_{ref} - V)). \end{aligned} \quad (5)$$

and the tracking error dynamics of controller C_1 is described by:

$$\dot{e} + Ke = 0 \tag{6}$$

with $e = V_{ref} - V$. Its time constant is given by $\tau = 1/K$, where K is the feedback gain of the controller C_1.

This state feedback controller was used for time-course control of membrane voltage, for blocking AP generation, and for annihilation of AP propagation along the axon.

2.4. Cascaded controller for control of ion channel activation/inactivation

In order to obtain direct control of sodium activation variables m and inactivation h, the above described state feedback controller C_1 was cascaded with an additional (optimal) controller C_2. The resulting cascaded feedback controller computes a current stimulus I_{inj} necessary to track a specified sodium activation and inactivation references (m_{ref} and h_{ref}, respectively). The cascaded control scheme allows optimal time-course control of the biophysical states governing action potential generation and propagation.

The block diagram of the cascaded controller is shown in Fig. 6. Controller C_2 determines the optimal membrane voltage U needed for tracking of the specified reference time courses m_{ref} and h_{ref} such that a given cost function J is minimized and that constraints on the controller output $U = V_{ref}$ are fulfilled. The controller C_1 is then used to ensure that the membrane voltage $V(t)$ equals $V_{ref}(t)$.

Implementation of controller C_2 is based on MPC, since constraints on the control signal and parameters defining the cost function can be chosen such that the resulting control signals will satisfy physiological constraints and mimic biological membrane voltage time courses.

MPC is a discrete-time linear feedback control strategy which yields finite horizon optimal control in presence of input and state constraints (Mayne, Rawlings, Rao, & Scokaert, 2000; Morari & Lee, 1999). In MPC, the cost function J to be minimized (Eq. (7)) is a function of three different parameters/weights: w^U is used to limit the energy of the control signal, $w^{\Delta U}$ to weight (punish) rapid changes in the control signal, and w^y to weight the contribution of the tracking error. The controller performance can be tuned by a proper choice of these three weights serving as controller parameters. Since the solution of minimizing J does not depend on the absolute magnitudes of these three weights, w^y was set to a unity vector in the following:

$$\begin{aligned} J = \sum_{i=0}^{p-1} & \left\| w^U U(k+i|k) \right\|^2 \\ & + \left\| w^{\Delta U} \Delta U(k+i|k) \right\|^2 \\ & + \left\| w^y (\boldsymbol{x}(k+i+1|k) - \boldsymbol{x}_{ref}(k+i+1)) \right\|^2. \end{aligned} \tag{7}$$

MPC predicts the future output of the system p (prediction horizon) time steps in advance. It then chooses a value of $U(k)$ which minimizes J without violating the constraints. This calculation is iteratively repeated at each time step.

Because prediction is based on a linear, time-invariant discrete-time model, the first-order differential equations for sodium activation m and inactivation h of the HH model were linearized around the state ($V = 20$ mV, $m = 0.37$, $h = 0.09$) for the MPC law calculation. Sampling with $T_s = 0.01$ ms then led to a discrete-time state-space model of the form:

$$x(k+1) = Ax(k) + bU(k), \tag{8}$$

where $\boldsymbol{x} = (m, h)^T$ is the state vector and $\boldsymbol{b}$ is the input vector. The membrane voltage $U(k)$ is a scalar input variable. Since $m(k)$ and $h(k)$ are uncoupled state variables, state matrix $\boldsymbol{A}$ is a diagonal matrix. This model was used for the design of the MPC controller.

Constraints on output U of controller C_2, on incremental change ΔU, and on the system outputs m and h were determined from biophysical considerations and simulations of the original HH equations (Table 1).

The effect of different settings of controller parameters w^U, $w^{\Delta U}$, w^y, and p on the controller performance was examined by performing simulations with different combinations of controller parameter values taken from a regularly sampled parameter subspace (Table 2).

Linearization is a common strategy to reduce a dynamic system to a form where standard control design techniques for linear systems can be applied. In

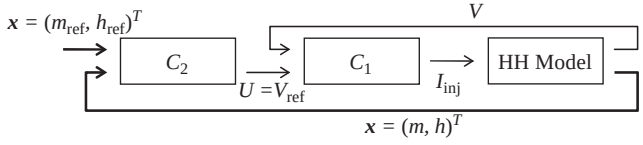

Fig. 6. Block diagram of the cascaded feedback controller for sodium activation m and inactivation h. Controller C_2 (MPC controller) calculates optimal $U = V_{ref}$ to track m_{ref} and h_{ref}, where the optimum is given by minimal cost function J. Controller C_1 (state feedback) determines I_{inj} to track V_{ref}. HH denotes the Hodgkin–Huxley model of the cell membrane with membrane voltage V.

Table 1
Constraints for controller C_2

Variable	Range
U	[−13.39, 122.04] mV
ΔU	[−82, 363] mV/ms
m, h	[0, 1]

The values of the constraints were obtained from HH model simulations by considering a scaling factor of 1.2.

Table 2
MPC Parameters used for simulations made with controller C_2

Variable	Increment	Range
w^U	0.05	[ε, 0.35]
$w^{\Delta U}$	0.5	[ε, 3.5]
p	5	[5, 20]

$\varepsilon = 2.2e{-}016$.

the model considered here, voltage-gated ion channels are the underlying biophysical mechanism of AP generation and propagation. For prediction, standard MPC requires a linearized internal model thereof. The effect of linearizing differential equations governing the opening and closing of voltage-gated ion channel as applied for the design of controller C_2 was investigated separately by comparing the response of the HH model to a current stimulus with the response of the model with a linearized differential equation for potassium activation n. Furthermore, a piecewise linear approximation consisting of two linearized submodels M_1 ($V_m = 0\,\text{mV}$, $n_0 = 0.32$) for $n < 0.35$ and M_2 ($V_m = 20\,\text{mV}$, $n_0 = 0.6191$) for $n \geqslant 0.35$ was evaluated. These simulations were used to determine if (piecewise) linearization changes the qualitative behavior of the overall system.

2.5. Evaluation of control-schemes

First, the state feedback controller C_1 was tested in its capability of controlling the membrane voltage i.e. it to impose reference time-courses on the membrane voltage V.

Second, the controller C_2 was used to control sodium ion channel activation and inactivation. Furthermore, the influence of the MPC controller parameters on the tracking ability of the controller C_2 was systematically examined. Two types of reference time-courses for the sodium channel dynamics were used for this analysis: the ones arising during the generation of an action potential (exact), and a simple, rectangular approximation thereof (switched). In the latter scheme, activation m_{ref} was switched from its steady state value $m = 0.05$ to 1.00 and inactivation h_{ref} was switched from $h = 0.60$ to 0.00 for a duration $\Delta T = 5\,\text{ms}$. By simulation, both the control signal U and the time courses of activation m and inactivation h were determined. Thereof, the corresponding root-mean-square (RMS) tracking errors of activation, $e_m = \text{RMS}(m_{\text{ref}} - m)$, and of inactivation, $e_h = \text{RMS}(h_{\text{ref}} - h)$, were computed.

Third, the state feedback controller was used to control (annihilate) action potential propagation in the multicompartment model.

3. Results

3.1. Control of membrane voltage

The feedback gain K of the state feedback controller C_1 was chosen to equal 10, as this value yielded an acceptable settling time and steady-state error while not using too large current amplitude. First, a step function was specified for reference voltage V_{ref}. Precise tracking was achieved. The resulting injected current I_{inj} and the tracking behavior are displayed in Fig. 7.

Then, signal waveforms of U as they arose in the cascaded control architecture as output of C_2 (see Section 3.2) were chosen as reference input V_{ref}. The top panels in Fig. 8 show tracking of V_{ref} for exact (as obtained in HH simulations) sodium (in-)activation time courses. The middle and bottom panels show tracking of V_{ref} for switched (in-)activation time courses for two different sets of MPC tuning parameters.

In presence of disturbances, open-loop action potential generation with a single current pulse can fail (for example, in the presence of other concurrent nerve activity/modulation), as shown in Fig. 9, where a periodic disturbance $d(t)$ was added to the membrane voltage ($d(t) = 30\ \sin(1.2t)$). This disturbance can be thought of as a model of current flowing into the cell body via the dendrites due to further synaptic connectivity of the neuron. This disturbance caused a firing-like behavior on its own.

In contrast, the cascaded feedback control scheme was able to efficiently suppress the disturbance (Fig. 10). The reference time course of V_{ref} was the output of C_2 for tracking exact (in-)activation. A comparison of the top and bottom row shows that increasing the feedback gain K led to an improved tracking performance. This ability of action potential generation in a cell with fluctuating membrane potential due to synaptic inputs is

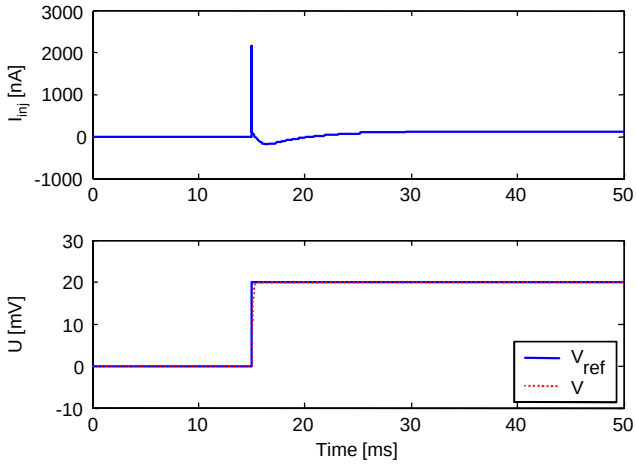

Fig. 7. State feedback controller C_1 used to track a rectangular membrane voltage reference time-course V_{ref}. Top: Controller output I_{inj}. Bottom: Reference V_{ref} and output V. V_{ref} and V almost coincide.

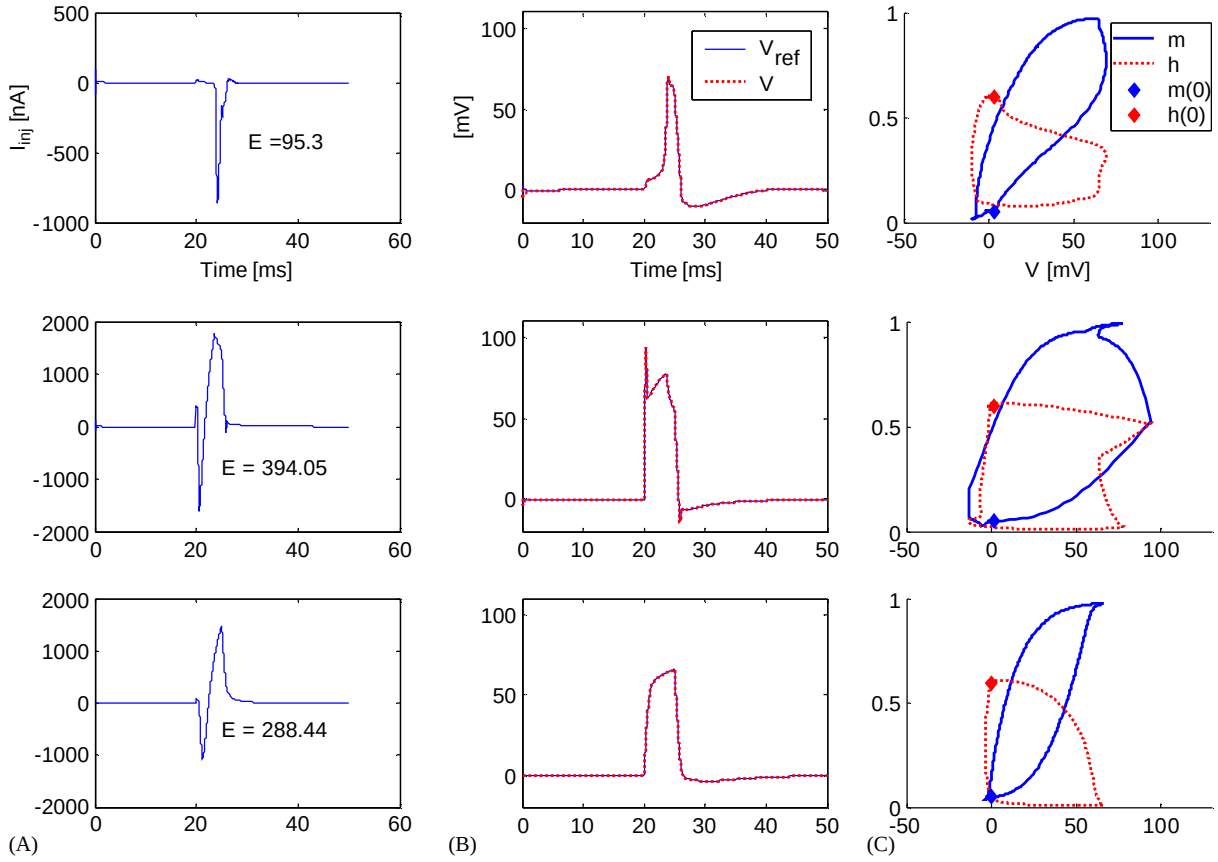

Fig. 8. Tracking of reference membrane voltage time-courses using controller C_1. The reference signals are the output signals of controller C_2. Controller output I_{inj} (A), membrane voltage V and reference time-course V_{ref} (B), two-dimensional phase subspace plot of membrane voltage V and sodium (in-)activation m and h (C). The energy of the control signal is denoted by E. Top: Tracking of membrane voltage time-course computed by C_2 for exact (in-) activation. Middle: Tracking of membrane voltage time-course as computed by C_2 ($w^U=\varepsilon$, $w^{\Delta U}=\varepsilon$, and $p=20$). The controller allows precise tracking of the reference signal which exhibits physiologically implausible rapid changes at the on- and offset under higher allowed cost (higher energy of the control signal). Bottom: Tracking of a physiologically more plausible membrane voltage reference time-course as computed by C_2 for a different set of tuning parameters ($w^U=\varepsilon$, $w^{\Delta U}=3.5$, and $p=20$). This leads to a smoother control signal. In all three cases, V_{ref} and V almost coincide.

a key feature of the suggested feedback control architecture since dense interconnectivity and resulting synaptic activity is a prevalent feature of biological neural systems.

3.2. Control of ion channel activation/inactivation

Control of ion channel activation and inactivation was based on a linearized model of the channel dynamics (Eq. (2)). Comparing the original model with the linearized model allows estimation of the linearization modeling error. The time-course of potassium activation variable during an action potential was compared to the case with a linearized and a piecewise linear potassium equation (Fig. 11). In the linear case, the action potential was of increased width, whereas the piecewise approximation mostly matched the original time-course (Panel A). The RMS difference value between the action potential generated by nonlinear vs. linearized models was much smaller for the piecewise linearized potassium activation (Panel B). However, actual action potential generation was unaffected by this linearization. Since the qualitative behavior of the linearized model matched the original nonlinear model, reasonable tracking performance of the MPC controller was expected.

Fig. 12A shows m, h, m_{ref}, and h_{ref} during tracking of the rectangular activation/inactivation reference inputs. In this case, the MPC parameters were set to $w^U=w^{\Delta U}=\varepsilon$ and $p=20$. Several possible reasons for the difference between activation and inactivation tracking error ($e_m=0.1089$ compared to $e_h=0.5456$) can be thought of. First, the approximation of the biophysical process of channel activation and inactivation with concurrently occurring rectangular pulses is not precise enough. Also, given only one control variable, membrane voltage U, and two dynamic states to control (m and h), the lack of one degree of freedom prevents the

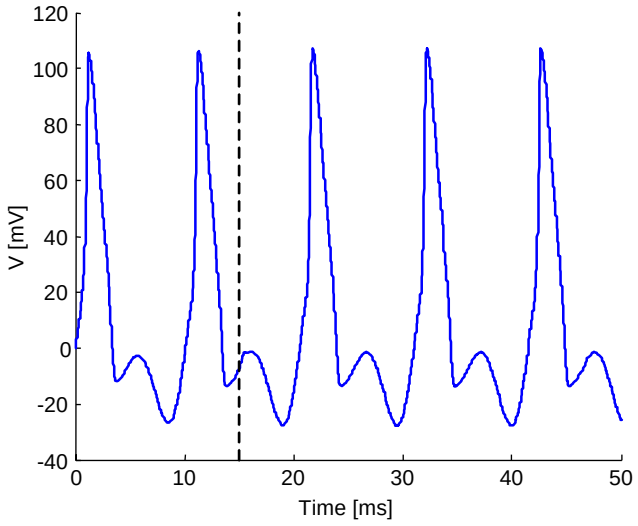

Fig. 9. Unsuccessful feedforward action potential generation in case of a periodic disturbance $d(t) = 30\sin(1.2t)$ added to the membrane voltage. The application of a rectangular current pulse at $t = 15$ ms (amplitude: 14 nA, duration: 0.5 ms, marked by a vertical dashed line) which was used to trigger an action potential in the absence of disturbances (Fig. 3) is not sufficient to elicit an action potential anymore. The neuron exhibits firing-like behavior on its one due to disturbance.

controller from precisely tracking the time-courses of both reference signals simultaneously (although the linearized system is controllable). If this is the case, individual tracking for either activation m or inactivation h should exhibit a significantly smaller tracking error than in the above-discussed case. Moreover, the model predictive controller is based on a linear model of the nonlinear state equations describing channel activation and inactivation. If the discrepancy between model and system to control is too big, decrease in tracking performance can be expected. The actual underlying cause for the difference in tracking error for activation and inactivation is probably a combination of both effects. For the case of tracking sodium inactivation time-course separately, an increase in tracking performance was observed but still a substantial tracking error remained (results not shown). This indicates that the mismatch between the actual nonlinear system governing sodium inactivation and the linearized model used for prediction by the MPC controller is at least partly responsible for the tracking error in h. Since tracking error for inactivation h was indeed decreased for tracking of inactivation alone, better tracking performance for more realistic reference time-courses was

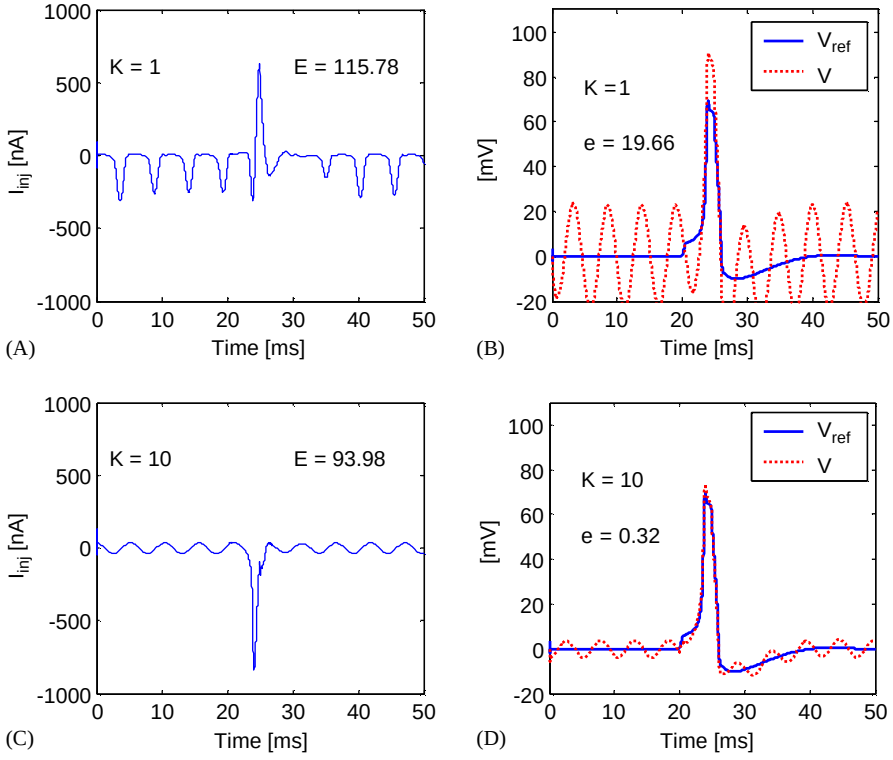

Fig. 10. Controller C_1: Tracking performance of reference V_{ref} (C_2 output for tracking of exact sodium (in-)activation with $w^U = \varepsilon$, $w^{\Delta U} = 3.5$, and $p = 20$) in case of external disturbance $d(t)=30\sin(1.2t)$ added to the membrane voltage V for two values of feedback gain $K \in \{1, 10\}$. Energy in controller signal and tracking error are denoted by E and e, respectively. Tracking for $K = 1$. Controller output I_{inj} (A). Membrane voltage V exhibits oscillatory component, however action potential generation by the disturbance as in the feedforward case (Fig. 9) is suppressed (B). Tracking for $K = 10$. Controller output I_{inj} (C). Membrane voltage V and reference V_{ref} (D).

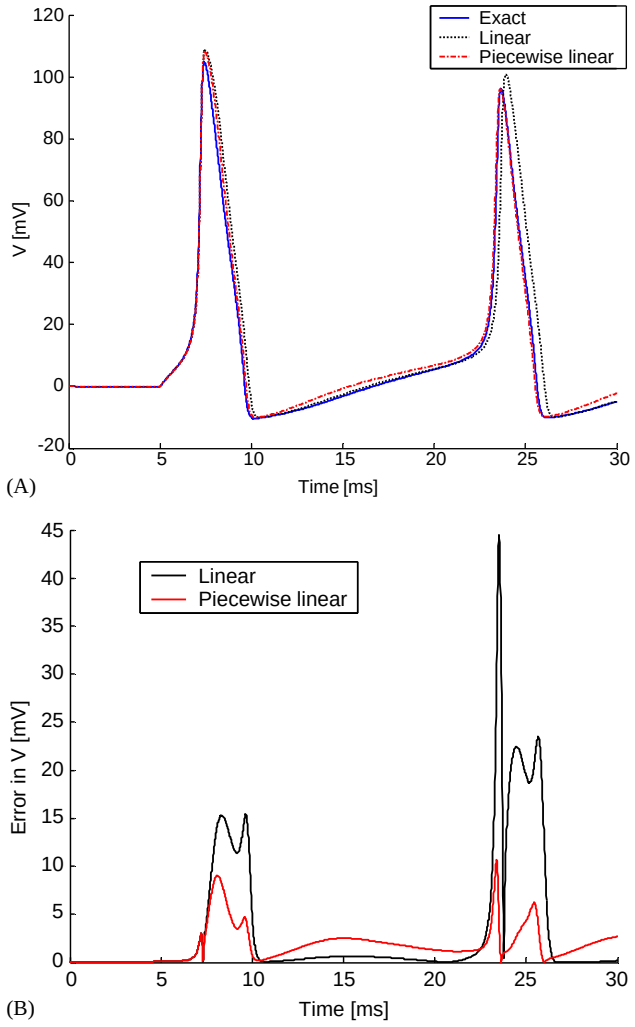

Fig. 11. Action potential generation by the use of exact, linear, and piecewise-linear differential equation for potassium activation n. In the linear case, the action potential is delayed and its width increased (A). These effects are less prominent when using the piecewise-linear approximation resulting in a decreased RMS error (deviation of the original AP obtained by the use of nonlinear differential equation for potassium activation n) (B).

expected. However, the slight modification of introducing a delay between onset of the activation and of the inactivation pulse to better mimic the actual biophysical processes during action potential generation in an uncontrolled nerve cell did not change the qualitative tracking behavior (Fig. 12B).

Cost function parameters can be used to shape the output of controller C_2. Fig. 12C indicates that increasing the weight on the rate of change, $w^{\Delta U}$, led to a smoother control signal. For $w^{\Delta U}=\varepsilon$, U showed fast transitions at the onset and offset of the rectangular reference signal (solid line). A smoother control signal was achieved by setting $w^{\Delta U}=3.5$ (dashed line).

For exact sodium (in-)activation time courses (Fig. 13A), the resulting control signal computed by the MPC control law resembled an action potential (Fig. 13B).

The tracking error depended on the choice of the cost function parameters. Fig. 14 shows the error e_m plotted as a function of the two MPC parameters $w^{\Delta U}$ and w^{U}. In panel A, the MPC prediction horizon p was set to 5, whereas in panel B p equaled 20. A comparison of the two plots reveals that increasing the prediction horizon enlarged the set of possible combinations of values for $w^{\Delta U}$ and w^{U} with low-tracking error of approximately 0.1 mV.

3.3. Annihilation of AP propagation with state feedback controller

The state feedback controller C_1 was also used to annihilate action potential propagation in a multicompartment model of an axon. A train of action potentials was generated by injecting a bias current into the first compartment (corresponding to the initial axonal compartment where action potentials are generated in absence of externally injected current for suprathreshold synaptic activity). The state feedback controller was used to control the time-course of the membrane voltage in the fifth compartment. This corresponds to a site in the middle of an axon and can be considered as a scheme to block action potential conduction in individual nerve fibers. The reference time course V_{ref} was set to a constant value below AP threshold.

Action potential propagation in presence of the current injected by the controller into the localized axonal compartment is shown in Fig. 15. The membrane voltage time-courses of all ten compartments are displayed. Although the reference membrane voltage V_{ref} was set such that the membrane voltage of the controlled compartment was forced to a value close to its equilibrium value (resting membrane voltage), switching off the controller caused immediate restart of the action potential propagation (Panel A). This is due to currents entering from the neighboring compartments. In order to sustain annihilation of AP propagation, the controller had to be permanently switched on (Panel B).

4. Discussion

In this paper, new approaches to control nonlinear nerve cell dynamics based on the HH equations were introduced and evaluated in simulations. Starting point was the study of the biophysical process of sodium ion channel activation and inactivation responsible for generation and propagation of APs. The developed control schemes were aimed at achieving feedback

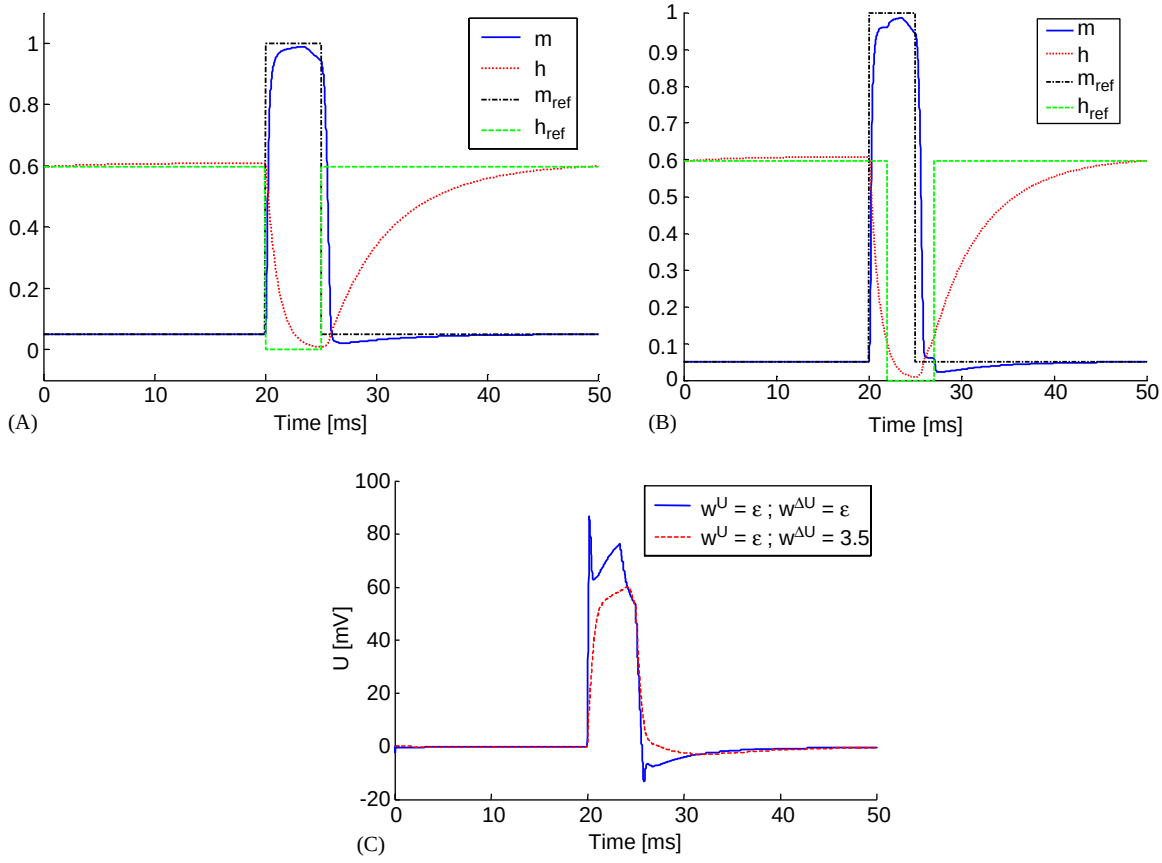

Fig. 12. Controller C_2. (A) Tracking rectangular reference time-course for sodium activation m_{ref} and inactivation h_{ref}, respectively (controller parameters: $w^U = w^{\Delta U} = \varepsilon$ and $p = 20$). (B) Tracking error of rectangular reference time-course for sodium activation and delayed sodium inactivation does not decrease compared to (A). (C) Output of controller C_2. Control signal U for tracking rectangular m_{ref} and h_{ref} with $w^U = \varepsilon$, $w^{\Delta U} = \varepsilon$, $p = 20$ (as in A, solid line) and $w^U = \varepsilon$, $w^{\Delta U} = 3.5$, $p = 20$ (dashed line). An increase of weight $w^{\Delta U}$ produced a smoother control signal, which qualitatively better corresponds to an action potential.

control of the time-courses of these state variables. Based on a nerve cell model consisting of coupled nonlinear differential equations, a cascaded control scheme was designed and investigated. The cascaded controller consisted of the state feedback controller accounting for the nonlinearities in the individual ionic currents, and the MPC controller. Potential applicability of this controller to annihilation of action potential generation and propagation was shown in this study.

To the knowledge of the authors, this is the first application of model-based feedback control in a study investigating electrical nerve cell stimulation. The study of electrical stimulation of nerve cell activity has a long history. Many existing nerve stimulation protocols are basically simple feedforward schemes where the exact dynamics of the biophysical states of the targeted neurons is disregarded. In contrast to such single pulse stimulation schemes, the cascaded controller combining state feedback and optimal control can be used to directly control the time-courses of the underlying biophysical variables. The channel dynamics are controlled in a closed-loop manner instead of directly injecting charge to affect the membrane voltage with the goal of reaching $V_m > V_{AP,threshold}$. Together with the explicit consideration of inherent nonlinearities and constraints on time-courses of the control signal, this study introduces a new conceptual framework for nerve cell stimulation and control.

In the presented work, the characteristics of the cascaded feedback controller as a function of the controller parameters were investigated. The choice of parameters describing the optimal controller affected both the tracking error and the control signal waveform. It was found that the weights of the cost function and the MPC constraints can be used to define a controller generating an output signal that fulfils physiological constraints, but offers greater freedom in its shape compared to the square pulse waveform that is

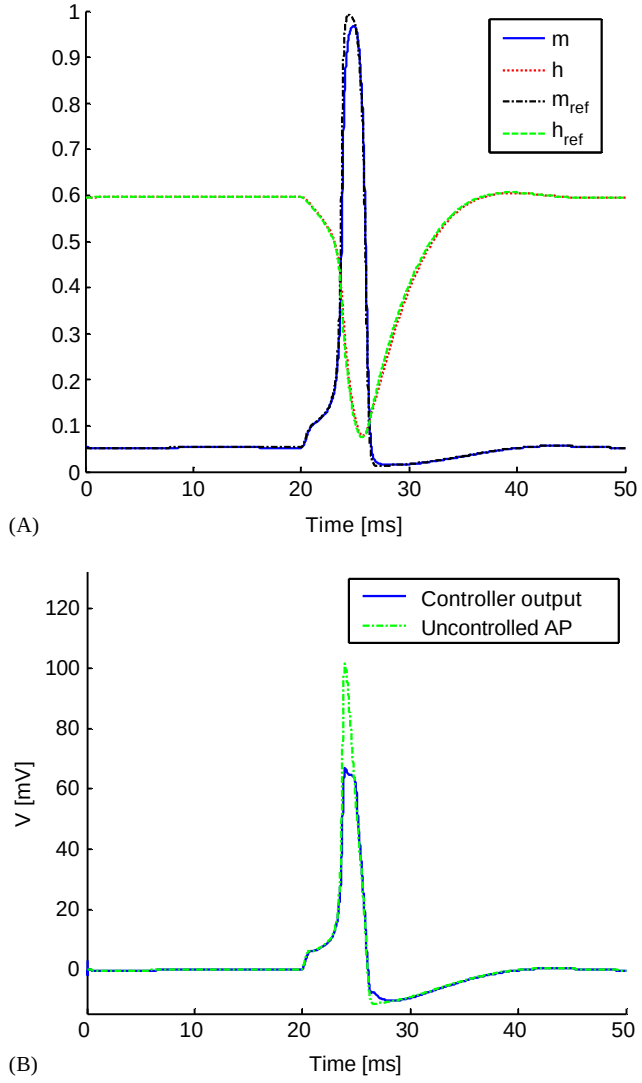

Fig. 13. Controller C_2. (A) Tracking of exact reference time-courses for sodium activation m_{ref} and inactivation h_{ref}, respectively. (B) Control signal U is compared to action potential of uncontrolled system. Qualitatively, the shape matches the controller output, however there is a clear difference in peak amplitude.

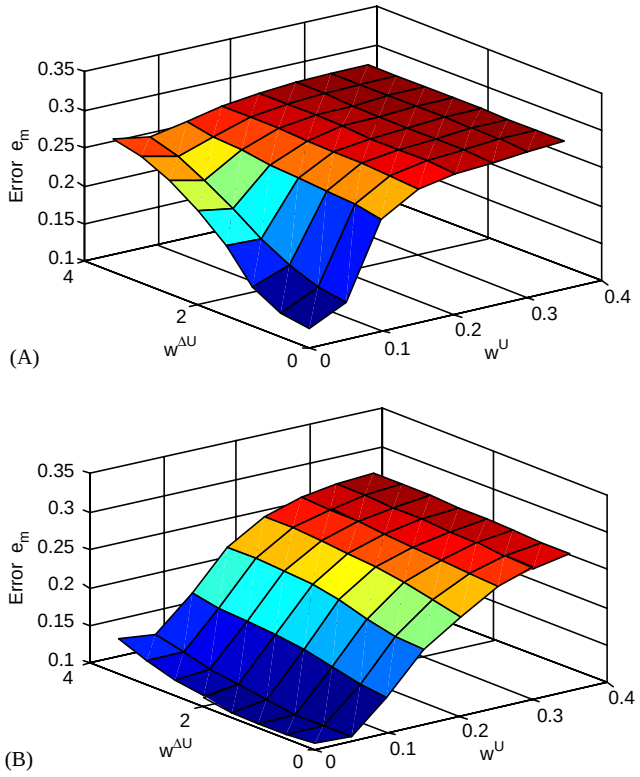

Fig. 14. Controller C_2. RMS tracking error e_m=RMS(m_{ref}, m) as function of controller parameter $w^{\Delta U}$ and w^{U} for two different values of prediction horizon $p \in \{5, 20\}$. For $p=5$, a nonzero value of either parameter leads to an increase of the tracking error (A). For $p=20$, the tracking error shows little dependence on the controller parameter $w^{\Delta U}$ for small values of w^{U} (B). Hence, an increase of the prediction horizon allows smoother changes in $V(w^{\Delta U} \gg \varepsilon)$ without substantial increase of e_m.

predominantly used nowadays. However, the computational complexity of the MPC controller and the required estimation/measurements of the state variables m, h, and V must be taken into account and may be the main obstacle when implementing feedback controllers introduced in this manuscript. A possibility of an offline computation of the MPC control law, as shown by Borelli (2002), might help to overcome some of the above-mentioned limitations.

The controller design is based on a neuron model which was first introduced by Hodgkin and Huxley (1952). The parameters of this model were chosen to fit data from experiments measuring the electrophysiological properties of the giant squid axon. It is the standard nerve cell model used in theoretical and simulation studies of neural dynamics that has been experimentally verified numerous times over the past 50 years. There exist specific extensions for other types of neurons; models of neurons from different species (including humans) as well as of different parts of the central nervous system exhibit very similar structure. It is possible to adapt the control law to account, for example, for additional ionic currents in more complex neuronal models. On the other hand, our study introduces control schemes to directly control the dynamics of sodium ion channels, which are responsible for action potential generation in most nerve cells.

Feedback control schemes based on time-course control of biophysical states in nerve cells might lead to the development of new electrical stimulation systems as neural prostheses for patients suffering from loss of function or aberrant electrical signal generation in the nervous system caused by accident or disease. For example, single cell stimulation is of major interest for suppression of undesired neural oscillation as it occurs in patients with Parkinson's disease or epilepsy (Durand & Bikson, 2001). The developed control schemes also

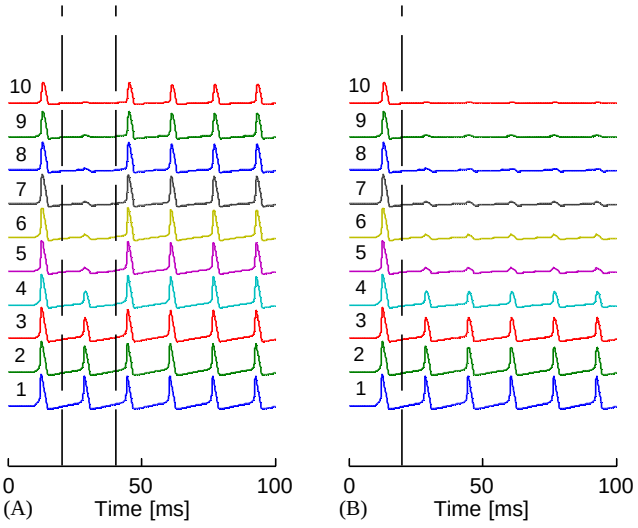

Fig. 15. Application of state feedback controller C_1 to suppress action potential propagation in a multicompartment model of an axon. Each trace represents the voltage time course in a given compartment. The individual compartments are coupled by a conductance. Controller C_1 is used to suppress action potential generation at the fifth compartment. Interval during which controller was switched on is delimited by vertical dashed lines. (A) Controller was switched on to drive the membrane voltage to its equilibrium value and switched off again. The action potential generation immediately rebounded since inflowing current from neighboring compartments depolarize the compartment above threshold. (B) In order to achieve action potential propagation block, the controller was kept switched on.

realize a new technique to block signal conduction in nerve fibers (as shown for the multicompartment model), whereby these techniques can be based on conditioned (switched) or unconditioned (continuous) stimulation regime. Possible applications are weakening or blocking of specific reflexes and annihilation of unwanted neural activity in different neural pathways. These are examples of where a device based on the introduced controllers for closed-loop control of nerve cell dynamics could be applied.

However, much work remains to be done before clinical studies can be considered. Stimulation devices implementing closed-loop control laws require further improvement in terms of computational power of the control modules and the interfaces measuring or estimating the biophysical states of the neural environment of the stimulation device. Open issues are also placement and stability of electrodes.

To conclude, novel feedback control schemes for the control of nerve cell dynamics were designed and evaluated in this study. This theoretical development is expected to further encourage control engineers to consider the manifold of interesting and challenging problems arising in the design of sophisticated electrical stimulation devices for rehabilitation of patients suffering from dysfunctions of the nervous system.

References

Borelli, F. (2002). *Discrete Time Constrained Optimal Control*. Ph.D. Thesis at Automatic Control Laboratory, Swiss Federal Institute of Technology, Zurich, Switzerland (http://control.ethz.ch).

Durand, D. M., & Bikson, M. (2001). Suppression and control of epileptiform activity by electrical stimulation: a review. *Proceedings of the IEEE*, *89*(7), 1065–1082.

Fröhlich, F., & Jezernik, S. (2004). Annihilation of single cell neural oscillations by feedforward and feedback control. *Journal of Computational Neuroscience*, *17*(2), 165–178 (September/October 2004).

Hodgkin, A. L., & Huxley, A. F. (1952). A quantitative description of membrane current and its application to conduction and excitation in nerve. *Journal of Physiology*, *177*, 500–544.

Kandel, E. R., Schwartz, J. H., & Jessel, T. M. (2000). *Principles of Neural Science* (Fourth ed). New York, NY: McGraw-Hill.

Khalil, H. K. (2002). *Nonlinear Systems* (Third ed). Upper Saddle River, NJ: Prentice Hall.

Koch, C. (1999). *Biophysics of computation: information processing in single neurons*. New York, NY: Oxford University Press.

Mayne, D. Q., Rawlings, J. R., Rao, C. V., & Scokaert, P. O. M. (2000). Constrained model predictive control: stability and optimality. *Automatica*, *36*(6), 789–814.

McNeal, D. R. (1976). Analysis of a model for excitation of myelinated nerve. *IEEE Transactions on Biomedical Engineering*, *23*(4), 329–337.

Morari, M., & Lee, J. H. (1999). Model predictive control: past, present and future. *Computers and Chemical Engineering*, *23*(4–5), 667–682.